JVI Accepted Manuscript Posted Online 10 July 2019
J. Virol. doi:10.1128/JVI.00679-19

Determination of critical requirements for NS2-3-independent virion formation of classical swine fever virus

D. Dubrau[a,#], S. Schwindt[a], O. Klemens[a,#], H. Bischoff[a,+] and N. Tautz[a,*]

[a]University of Luebeck, Institute of Virology and Cell Biology, Luebeck, Germany

Running Head: Determinants for NS2-3-independent virion formation of CSFV

*Address correspondence to: norbert.tautz@vuz.uni-luebeck.de
University of Luebeck, Institute for Virology and Cell Biology
Ratzeburger-Allee 160, D-23562 Luebeck, Germany
Phone: +49 451 3101 4000; Fax: +49 451 3101 4004

[#]Present address: EUROIMMUN AG, Luebeck, Germany
[+]Present address: AniCon Labor GmbH, Hoeltinghausen, Germany

Key words: CSFV, pestivirus, NS2-3-independent virion morphogenesis, positive strand RNA virus, NS3/4A

Abstract

For members of the *Flaviviridae* it is known that beside the structural proteins also nonstructural (NS) proteins play a critical role in virion formation. Pestiviruses such as bovine viral diarrhea virus (BVDV) rely on uncleaved NS2-3 for virion formation while its cleavage product NS3 is selectively active in RNA replication. This dogma was recently challenged by the selection of gain-of-function mutations in NS2 and NS3 which allowed virion formation in absence of uncleaved NS2-3 in BVDV-1 variants encoding either an ubiquitin (NS2-Ubi-NS3) or an IRES (NS2-IRES-NS3) between NS2 and NS3. To determine whether the ability to adapt to NS2-3-independent virion morphogenesisis is conserved among pestiviruses, we studied the corresponding NS2 and NS3 mutations (2/T444-V and 3/M132-A) in classical swine fever virus (CSFV). We observed that these mutations were only capable of restoring low level NS2-3-independent virion formation for CSFV NS2-Ubi-NS3. Interestingly, a second NS2 mutation (V439-D) identified by selection was essential for high titer virion production. Similar to previous findings for BVDV-1, these mutations in NS2 and NS3 allowed only for low titer virion production in CSFV NS2-IRES-NS3. For efficient virion morphogenesis additional exchanges in NS4A (A48-T) and NS5B (D280-G) were required, indicating that these proteins cooperate in NS2-3-independent virion formation. Interestingly, both NS5B mutations, selected independently for NS2-IRES-NS3 variants of BVDV-1 and CSFV, are located in the fingertip region of the viral RdRp, classifying this structural element as a novel determinant for pestiviral NS2-3-independent virion formation. Together, these findings will stimulate further mechanistic studies on genome packaging of pestiviruses.

48 **Importance**

49 For *Flaviviridae* members the nonstructural proteins are essential for virion formation
50 and thus exert a dual role in RNA replication and virion morphogenesis. However, it
51 remains unclear how these proteins are functionalized for either process. In wild-type
52 pestiviruses the NS3/4A complex is selectively active in RNA replication, while NS2-
53 3/4A is essential for virion formation. Mutations recently identified in BVDV-1 rendered
54 NS3/4A capable of supporting NS2-3-independent virion morphogenesis. A comparison
55 of NS3/4A complexes incapable/capable of supporting virion morphogenesis revealed
56 that changes in NS3/NS4A surface interactions are decisive for the gain-of-function.
57 However, so far the role of the NS2 mutations as well as the accessory mutations
58 additionally required in the NS2-IRES-NS3 virus variant have not been clarified. To
59 unravel the course of genome packaging, the obtained additional sets of mutations for a
60 second pestivirus species (CSFV) are of significant importance to develop mechanistic
61 models for this complex process.

Introduction

The family *Flaviviridae* comprises the genera *Flavivirus*, *Hepacivirus*, *Pestivirus* and *Pegivirus* (1). The pestiviral positive-strand RNA genome is translated into one polyprotein which is processed by cellular and virus-encoded proteases (2). The structural proteins are located in the N-terminal third while most of the nonstructural proteins reside in the C-terminal two thirds of the polyprotein. The order of the proteins in the polyprotein is: NH_2-N^{pro} (N-terminal protease), C (capsid protein, core), E^{rns} (envelope protein RNase secreted), E1, E2, p7, NS2-3 (NS2, NS3), NS4A, NS4B, NS5A, and NS5B-COOH. The formation of infectious virions involves besides the structural proteins also the nonstructural (NS) proteins (3). For pestiviruses the involvement of all NS proteins in virion morphogenesis except for N^{pro} and NS4B has been established (4-9). Since NS4B is critically involved in virion morphogenesis of HCV (10, 11), a similar function is to be assumed for its pestiviral counterpart. NS3 is a multifunctional protein which has serine protease function as well as helicase and NTPase activities (12, 13). Only in complex with NS4A, NS3 exerts its full protease activity which is generating the C terminus of NS3 and catalyzes all downstream cleavages. NS4A consists of an N-terminal transmembrane domain (TM), a central peptide, a kink domain and a C-terminal acidic domain. The TM is most likely responsible for anchoring the NS3/4A complex to intracellular membranes. The central peptide forms a beta sheet which intercalates into the N-terminal beta-barrel domain of the NS3 serine protease domain (14).

For the members of the genus *Pestivirus*, like bovine viral diarrhea virus (BVDV) or classical swine fever virus (CSFV) a complex regulation of their RNA replication has been observed which is required for the ability of these viruses to establish persistent infections by intra uterine infection of the fetus (2, 15). On cellular level, nonstructural protein 2-3 (NS2-3) is efficiently cleaved into NS2 and NS3 in the early phase of

88 infection (15). NS3 represents an essential component of the RNA replication
89 complex (16). The NS2 autoprotease, which is catalyzing the NS2-3 cleavage,
90 depends in its activity on a stable interaction with the cellular chaperone DNAJC14
91 that is only available in low quantities in cells (15, 17). Thus, when translation of viral
92 proteins advances no sufficient amount of this cellular cofactor is available and
93 uncleaved NS2-3 accumulates in the infected cell. The regulation of viral RNA
94 replication mediated by DNJC14 dependent NS2-3 cleavage has been verified for a
95 broad range of pestiviruses (18). NS2-3 is strictly required for virion formation and
96 can in this function not be replaced by NS2 and NS3 (5). This represents a
97 fundamental difference to the hepatitis C virus (HCV) system where it has been
98 demonstrated that uncleaved NS2-3 is not essential for virion formation (19, 20).
99 Recently, it has been shown that BVDV-1 can be adapted to a HCV-like packaging
100 scheme in which NS2 and NS3 can functionally substitute uncleaved NS2-3 in virion
101 morphogenesis (21). The success of this approach was based on the use of cDNA
102 fragments derived from the natural cytopathogenic BVDV-1 strain Osloss, which
103 encodes a host cell-derived ubiquitin monomer between NS2 and NS3 (22). This
104 virus, for which no infectious cDNA has been established so far, contains in
105 retrospection all mutations required for virion morphogenesis in the absence of
106 uncleaved NS2-3. The mutations essential and sufficient for this phenotype could be
107 narrowed down in the context of strain NCP7 to one amino acid exchange in NS2
108 (E440-V, named 2/EV) and one in NS3 (V132-A, named 3/VA)(23). While these two
109 mutations allowed for efficient NS2-3-independent virion formation of a monocistronic
110 BVDV encoding an ubiquitin gene between NS2 and NS3, a bicistronic BVDV
111 genome with an EMCV-IRES between the genes coding for NS2 and NS3, depends
112 on additional mutations in E2, NS2 and NS5B for efficient packaging (23). Further
113 structural and biochemical characterization identified the NS3 position 132 as a

114 crucial determinant in the coordination of the NS3 surface interaction with the NS4A
115 kink region (14). To be functional in RNA replication a stable surface interaction
116 between the NS4A kink region and NS3 is mandatory. In contrast, a more flexible
117 NS3/4A complex conformation with a less tightly bound C-terminal part of NS4A is a
118 requirement for virion morphogenesis. On the molecular level this effect is achieved
119 by exchange 3/VA in BVDV-1 NS3 which weakens the interaction between NS3 and
120 the kink region of NS4A (14). While this explains the effect of the gain-of-function
121 mutation identified in NS3, the role of the exchange 2/EV in NS2 is ill-defined and
122 currently under investigation. The same applies to the accessory mutations which are
123 additionally required for high titer virion formation when an EMCV-IRES instead of an
124 ubiquitin-coding sequence is inserted between the NS2 and NS3 genes. For BVDV-1
125 these accessory mutations comprise the insertion of a lysine in E2 downstream of
126 amino acid 214, exchange T269-A in NS2 and the mutation E145-G in NS5B (23).
127 In the present study we investigated whether the requirements for NS2-3-
128 independent virion morphogenesis are conserved among pestiviruses. To this end,
129 the sets of gain-of-function mutations necessary and sufficient to rescue virion
130 morphogenesis in CSFV mutants NS2-Ubi-NS3 and NS2-IRES-NS3 were
131 determined and we could demonstrate that a second pestivirus species can also
132 adapt to virion morphogenesis in the absence of uncleaved NS2-3 by only a few
133 amino acid exchanges. Furthermore this study broadens the spectrum of mutations
134 outside of the NS2-3 region which facilitate NS2-3-independent virion formation.
135 Interestingly, in both virus species mutations in the same structural element of NS5B
136 are supporting this process. The obtained data will significantly stimulate further
137 studies aiming at unraveling the molecular basis of virion morphogenesis in
138 pestiviruses.
139

Results

The amino acid exchanges T444-V in NS2 (2/TV) and M132-A in NS3 (3/MA) allow the formation of infectious CSFV in absence of uncleaved NS2-3 at very low titers. Previously, it was demonstrated for a BVDV-1 NS2-Ubi-NS3 mutant that two amino acid exchanges, one in NS2 (E440-V, 2/EV) and one in NS3 (V132-A, 3/VA), were sufficient to rescue efficient virion morphogenesis (23). To determine whether the requirements for NS2-3-independent virion morphogenesis are conserved among pestiviruses we generated cDNA clones of CSFV strain Alfort/Tuebingen in which the coding sequences for NS2 and NS3 were separated by either an ubiquitin gene or by insertion of the internal ribosomal entry site (IRES) of encephalomyocarditis virus (EMCV). These cDNA clones were named pCSFV NS2-Ubi-NS3 or pCSFV NS2-IRES-NS3, respectively (see Fig. 1A for schemes of the encoded viral genomes). To ensure the retention of the Ubi/IRES-insertion for the production of free NS3, thereby rendering them essential for RNA replication, the NS2 protease was inactivated by the deletion of the active site cysteine (ΔC380) (see Materials and Methods). In these cDNA clones we introduced the corresponding mutations for CSFV which are T444-V in NS2 - (2/TV) and M132-A in NS3 ((3/MA), , resulting in mutant viruses CSFV NS2-Ubi-NS3 (2/TV, 3/MA) and CSFV NS2-IRES-NS3 (2/TV, 3/MA) (Fig. 1A). *In vitro* transcribed RNA of these CSFV full-length genome derivatives as well as CSFV wild-type (WT) and the RNA replication-deficient control CSFV (5B/GAA) were electroporated into SK6 cells and RNA replication competence was monitored indirectly by NS3-specific immunofluorescence (IF) staining 24 h post electroporation (pe) (Fig. 1B, top panel – RNA replication). NS3-positive cells were detected for CSFV wild-type (WT) as well as for the derivatives CSFV NS2-Ubi-NS3 and CSFV NS2-IRES-NS3 either without or with mutations 2/TV and 3/MA (Fig. 1B, top panel – RNA replication). As expected,

166 no NS3-positive cells were detected for the RNA replication-deficient negative control
167 CSFV (5B/GAA) (Fig. 1B, top panel – RNA replication).
168 Cell culture supernatants were harvested 48 h pe and the infection status of the
169 electroporated cells was analyzed by NS3-IF (Fig. 1B, middle panel – virus
170 propagation). Effective spread was observed for CSFV WT as almost all cells were
171 NS3-positive. Since CSFV WT replication is noncytopathogenic no decrease of cell
172 numbers was observed. In contrast, only a small number of NS3-positive cells was
173 detected at 48 h pe of CSFV NS2-Ubi-NS3/(2/TV, 3/MA) and CSFV NS2-IRES-
174 NS3/(2/TV, 3/MA) indicating that all these virus variants display very inefficient
175 spread in cell culture (Fig. 1B, middle panel – virus propagation). When comparing
176 24 h pe and 48 h pe a severe reduction of NS3-positive cells was observed for CSFV
177 NS2-Ubi-NS3/(2/TV, 3/MA) and CSFV NS2-IRES-NS3/(2/TV, 3/MA), which is due to
178 the cytopathogenic replication phenotype of this kind of viral genomes with
179 deregulated NS3 expression (6, 14, 23).
180 To analyze for the production of infectious virions cell culture supernatants were
181 harvested at 48 h pe and 500 µl of those supernatants were used to inoculate naïve
182 SK6 cells (Fig. 1B, lower panel – infection). 72 h post infection (pi) infected cells were
183 indirectly detected by NS3-IF. As expected, almost all cells were NS3-positive in the
184 case of CSFV WT infection. In contrast, only a few NS3-positive cells were detected
185 after inoculation of SK6 cells with CSFV NS2-Ubi-NS3 (2/TV, 3/MA) while inoculation
186 with CSFV NS2-IRES-NS3 (2/TV, 3/MA) yielded no detectable infected cells, which
187 indicates a limited or impaired competence in virion formation. These results were
188 confirmed by viral titer analyses of cell culture supernatants which were harvested at
189 48 h pe, as the tissue culture infection dose per ml ($TCID_{50}$/ml) of CSFV NS2-Ubi-
190 NS3 (2/TV, 3/MA) was 1.4×10^2 while CSFV NS2-IRES-NS3 (2/TV, 3/MA) produced
191 no titers (Fig. 1C). Efficient virion formation of CSFV WT was observed with titers of

192 about 2.2 x 10^6 $TCID_{50}$/ml (Fig. 1C). In line with previous results, no infected cells
193 and no viral titers were observed for CSFV NS2-Ubi-NS3 and CSFV NS2-IRES-NS3
194 (6). To control for the efficiency of NS2-ubi-NS3 cleavage a western blot analysis
195 was performed (Fig. 1D). No uncleaved NS2-ubi-NS3 was detected in cells
196 electroporated with either CSFV NS2-ubi-NS3 coding RNA confirming efficient
197 cleavage by cellular ubiquitin hydrolases. In contrast, in the cells electroporated with
198 wild type CSFV RNA which are used as control, uncleaved NS2-3 is readily detected.
199 However, it must be pointed out, that NS2-3 is about 7 kDa smaller than the NS2-ubi-
200 NS3 encoded by the mutant viruses used throughout the study.
201
202 **Efficient NS2-3-independent virion formation of CSFV NS2-IRES-NS3 depends**
203 **on additional mutations in NS2, NS4A and NS5B.** Based on the observation of
204 very low titers for CSFV NS2-Ubi-NS3 and CSFV NS2-IRES-NS3 in presence of
205 mutations 2/TV and 3/MA, a cell culture-based adaptation approach was applied to
206 identify additional mutations which enhance virion formation. In this experimental
207 setup, CSFV NS2-IRES-NS3 (2/TV, 3/MA) was used for serial cell culture passaging
208 since this derivative exhibits a more stringent separation of NS2 and NS3 compared
209 to CSFV NS2-Ubi-NS3. Moreover, similar approaches have been successfully used
210 in previous studies concerning NS2-3-independent virion formation of BVDV (21, 23).
211 Accordingly, CSFV NS2-IRES-NS3 (2/TV, 3/MA) RNA was electroporated into SK6
212 cells followed by serial cell culture passages (Fig. 2A, top panel). Electroporated cells
213 were passaged until higher percentages of NS3-positive cells as well as an increased
214 cytopathic effect (CPE) could be observed. Thereafter, cell culture supernatants were
215 passaged until high numbers of NS3-positive cells and increased CPE were
216 observed after infection. A total of 11 passages (6 cell passages and 5 passages of
217 cell culture supernatants) were performed. Inoculation with the resultant cell culture

supernatant led to large numbers of NS3-positive cells as well as a severe CPE, indicating efficient virion morphogenesis of the adapted variant of CSFV NS2-IRES-NS3 (2/TV, 3/MA) (data not shown). After this selection process the virus was biologically cloned (i.e., "CSFV NS2-IRES-$NS3_{sc}$") and was shown to reach a titer of about 2.3 x 10^6 $TCID_{50}$/ml in the cell culture supernatant confirming enhanced packaging competence of CSFV NS2-IRES-$NS3_{sc}$. Subsequently, CSFV NS2-IRES-$NS3_{sc}$ was used to infect naïve SK6 cells followed by isolation of viral RNA and sequence determination by RT-PCR. Direct sequencing followed by sequence analyses confirmed the retention of the initial mutations present in CSFV NS2-IRES-NS3 (2/TV, 3/MA) and revealed the presence of 7 additional second site mutations in CSFV NS2-IRES-$NS3_{sc}$ (Table 1 and Figure 2A, middle panel).

6 mutations led to the amino acid exchanges E1/AT, 2/QK, 2/VD, 3/LI, 4A/A48-T and 5B/DG, while one mutation was silent (Table 1). The fact that the initially introduced mutations 2/TV and 3/MA were retained in CSFV NS2-IRES-$NS3_{sc}$ suggested that they are critical for NS2-3-independent virion formation.

To determine whether this panel of second site mutations identified in CSFV NS2-IRES-$NS3_{sc}$ is improving NS2-3-independent virion formation, the cDNA clone CSFV NS2-IRES-$NS3_{8\text{-}mut}$ encoding the mutations 2/TV and 3/MA as well as the 6 additional amino acid exchanges was generated (Fig. 2A, middle). SK6 cells were electroporated with RNA *in vitro* transcribed from pCSFV NS2-IRES-$NS3_{8\text{-}mut}$ followed by titer analysis at 48 h pe. CSFV NS2-IRES-$NS3_{8\text{-}mut}$ reached titers of about 1.8 x 10^6 $TCID_{50}$/ml confirming the observed titer enhancing effect of the selected mutations (Fig. 2B). Infection at a defined multiplicity of infection (MOI) of 0.1 resulted in viral titers of about 2.0 x 10^6 $TCID_{50}$/ml at 72 h post infection (pi) (Fig. 2B).

To dissect which of these mutations is contributing to efficient NS2-3-independent virion formation, each of the mutations was omitted individually from pCSFV NS2-IRES-NS3$_{8\text{-mut}}$, creating a panel of eight different pCSFV NS2-IRES-NS3 derivatives. Their respective RNA transcripts were electroporated into SK6 cells and viral titers were determined 48 h pe and 72 h pi (MOI 0.1) (Fig. 2B). Since the individual absence of E1/AT, 2/QK and 3/LI had no or only marginal effects on viral titers, e.g. reductions of no more than 0.5 $\log_{10}$ $TCID_{50}$/ml at 48 h pe or 72 h pi (MOI 0.1), a major role of those mutations in NS2-3-independent virion formation was excluded (Fig. 2B). In contrast, crucial importance was confirmed for 2/VD, 2/TV and 3/MA since dramatically decreased titers of about 1.9 x 10^2 - 4.3 x 10^3 $TCID_{50}$/ml at 48 h pe were observed when one of these exchanges was omitted (Fig. 2B). A functional importance in NS2-3-independent virion formation of CSFV NS2-IRES-NS3 could be also detected for 4A/A48-T and 5B/DG, as their individual omission from CSFV NS2-IRES-NS3$_{8\text{-mut}}$ reduced viral titers by about one $\log_{10}$ $TCID_{50}$/ml (Fig. 2B). According to those results, it was hypothesized that CSFV NS2-IRES-NS3$_{5\text{-mut}}$ (Fig. 2A, bottom panel), encoding the mutations 2/VD, 2/TV, 3/MA, 4A/A48-T and 5B/DG (CSFV NS2-IRES-NS3$_{5\text{-mut}}$), is encoding a set of mutations sufficient for efficient NS2-3-independent virion formation. To test this hypothesis, RNA transcripts from pCSFV NS2-IRES-NS3$_{5\text{-mut}}$ were electroporated into SK6 cells and virion formation was determined. Titers of about 2.0 x 10^6 $TCID_{50}$/ml at 48 h pe and 72 h pi (MOI 0.1) were obtained, confirming this CSFV NS2-IRES-NS3 variant being able to support efficient NS2-3-independent virion formation. A parallel infection of SK6 cells with CSFV WT, CSFV NS2-IRES-NS3$_{sc}$, CSFV NS2-IRES-NS3$_{8\text{-mut}}$ and CSFV NS2-IRES-NS3$_{5\text{-mut}}$ at MOI 0.1 demonstrated that the latter cDNA derived virus clones reached a titer similar to the one of CSFV WT, demonstrating the fitness of these mutants (Fig. 2C).

268 Since the amino acid exchanges 3/MA, 4A/A48-T and 5B/DG promote efficient
269 formation of CSFV NS2-IRES-NS3, it was possible that those mutations are
270 modulating polyprotein processing and/or are enhancing RNA replication. To address
271 these aspects the bicistronic cDNA reporter construct pCSFV Bici RLuc IRES-Ubi-
272 NS3-3' was established which encodes N^{pro} and *Renilla* luciferase in the first open
273 reading frame (ORF) while the viral replicase proteins NS3-5B are generated from
274 the second ORF (Fig. 3).
275 Both processes could be independently assayed with the bicistronic reporter replicon
276 CSFV Bici RLuc IRES-Ubi-NS3-3': While an RNA transcript of the second ORF can
277 be individually generated by T7 RNA polymerase, allowing polyprotein processing
278 analyses in a replication-independent manner (Fig. 3A, upper panel), the replication-
279 competent replicon RNA can be transcribed from the same cDNA plasmid using SP6
280 RNA polymerase (Fig. 3C, upper panel). Variants of CSFV Bici RLuc IRES-Ubi-NS3-
281 3' encoding the mutations 3/MA, 4A/A48-T and 5B/DG as well as a replication-
282 deficient negative control 5B/GAA were generated and polyprotein processing as well
283 as RNA replication efficacies were determined by Western blotting or luciferase
284 assay, respectively (Fig. 3A and 3C).
285 A replication-independent approach was applied to analyze whether the mentioned
286 amino acid exchanges influence polyprotein processing (Fig. 3A). Huh7-T7 cells
287 were infected by vaccinia virus MVA/$T7^{pol}$ and transfected with plasmids pCSFV Bici
288 RLuc IRES-Ubi-NS3-3' and its derivatives. A derivative encoding the NS3/4A serine
289 protease inactivating mutation 3/S163-A served as control. Western blot analyses
290 with antibodies against NS3, NS4A, NS4B, NS5A and NS5B revealed authentic
291 polyprotein processing for the CSFV Bici RLuc IRES-Ubi-NS3-3' variants encoding
292 3/MA, 4A/A48-T or 5B/DG compared to the wild-type construct (Fig. 3B). Mutation
293 4A/A48-T interfered with NS4A detection by the NS4A-specific monoclonal antibody.

294 However, also for this mutant authentic polyprotein processing was indicated by the
295 NS3- and NS4B-specific Western blots (Fig. 3B).
296 CSFV Bici RLuc IRES-Ubi-NS3-3' replicon RNAs encoding the mutations 3/MA,
297 4A/A48-T and 5B/DG as well as a replication-deficient negative control 5B/GAA were
298 electroporated into SK6 cells and analyzed by luciferase assay (Fig. 3C, bottom
299 panel). As expected, luciferase activities of the replication-deficient negative control
300 5B/GAA declined over time while luciferase levels of wild-type CSFV Bici RLuc IRES-
301 Ubi-NS3-3' increased at 24 h pe to 8.4 x 10^6 relative light units (RLUs) compared to
302 the 2 h pe value followed by a decrease to 2.2 x 10^6 RLUs at 48 h pe, due to known
303 cytotoxic effects of those kind of replicons (4, 14, 23). Luciferase activities similar to
304 those detected after electroporation of the WT replicon were obtained for the 3/MA
305 variant and slightly reduced values for derivatives 4A/A48-T and 5B/DG excluding a
306 major impact of those mutations on RNA replication (Fig. 3D).
307
308 **The amino acid exchange 2/VD is critically required for efficient packaging of**
309 **CSFV NS2-Ubi-NS3.** To test whether the identified titer enhancing mutations 2/VD,
310 4A/A48-T and 5B/DG would also improve packaging efficiencies of the monocistronic
311 CSFV NS2-Ubi-NS3 (2/TV, 3/MA) variant, the respective derivative CSFV NS2-Ubi-
312 $NS3_{5\text{-mut}}$ encoding 2/VD, 2/TV, 3/MA, 4A/A48-T and 5B/DG was generated (Fig. 4A).
313 Titer analyses of cell culture supernatants collected at 48 h pe and 72 h after
314 infection at MOI 0.1 confirmed efficient formation of CSFV NS2-Ubi-$NS3_{5\text{-mut}}$ with
315 titers of about 3.2 x 10^5 $TCID_{50}$/ml at 48 pe and 9.3 x 10^7 $TCID_{50}$/ml at 72 h pi (MOI
316 0.1) (Fig. 4B).
317 To test whether all identified titer enhancing mutations, e.g. 2/VD, 4A/A48-T and
318 5B/DG, were required for optimal virion formation of CSFV NS2-Ubi-NS3, variants of
319 CSFV NS2-Ubi-$NS3_{5\text{-mut}}$ were generated in which individual amino acid exchanges

were absent (Fig. 4B). This approach revealed that in the monocistronic context of CSFV NS2-Ubi-NS3 the mutations 4A/A48-T and 5B/DG did not contribute to efficient NS2-3-independent virion formation since their absence had no negative impact on viral titers at 48 h pe or 72 h pi (MOI 0.1) (Fig. 4B). However, mutations 2/VD, 2/TV and 3/MA were highly critical in the context of CSFV NS2-Ubi-NS3, as dramatic decreases in viral titers were observed at 48 h pe when one of these mutations was absent (Fig. 4B). To control for the efficiency of NS2-ubi-NS3 cleavage a western blot analysis was performed (Fig. 4C).

Previous experiments on BVDV-1 have shown that the two mutations in NS2 and NS3, sufficient for the rescue of NS2-3-independent virion formation in monocistronic BVDV-1 NS2-Ubi-NS3, were not sufficient to allow for high titer virus production in the bicistronic BVDV-1 NS2-IRES-NS3 (23). In this study, a third mutation located in NS2 (2/VD) was found highly critical for CSFV NS2-Ubi-NS3 . To determine whether these 3 mutations are also sufficient to rescue virion formation in the context of the bicistronic CSFV NS2-IRES-NS3, we finally generated pCSFV NS2-IRES-NS3$_{3\text{-mut}}$ encoding the mutations 2/VD, 2/TV and 3/MA. After the electroporation of RNAs transcribed from this construct and from pCSFV NS2-Ubi-NS3$_{5\text{-mut}}$ into SK6 cells, viral titers were determined at 48 h pe (Fig. 4D). While the titers of CSFV NS2-IRES-NS3$_{5\text{-mut}}$ were about 2.0 x 10^6 $TCID_{50}$/ml, the titers of CSFV NS2-IRES-NS3$_{3\text{-mut}}$ reached only 1.4 x 10^3 $TCID_{50}$/ml, demonstrating that mutations A48-T in NS4A and D280-G in NS5B are essential for efficient virion production in the context of bicistronic CSFV NS2-IRES-NS3.

In contrast to alanine exchanges at positions L45 or Y47 in the NS4A kink region NS4A A48-T is unable to functionally substitute mutation 3/MA. As shown in Fig. 4, CSFV NS2-Ubi-NS3$_{5\text{-mut}}$ which contains mutations 3/MA as well as

346 NS4A/A48-T is efficient in virion production (Fig. 4). For BVDV-1 it was shown that
347 the alanine exchange at NS3 position 132 modulates the NS3/4A-kink interaction,
348 since this amino acid is part of the interaction interface between the surface of the
349 NS3 protease domain and the NS4A kink region, involving NS4A amino acids L45
350 and Y47 (Fig. 5A) (Dubrau et al., 2017). The data presented in Fig. 4 demonstrate
351 that mutation 3/MA is essential in the context of CSFV NS2-Ubi-NS3 at least in
352 clones which do not contain mutation 4A/A48-T. Based on the findings in the BVDV
353 system we decided to verify whether mutation 4A/A48-T, located in the NS4A kink-
354 domain, can functionally substitute mutation 3/MA. Accordingly, we generated the
355 mutants CSFV NS2-Ubi-NS3 (2/VD, 2/TV, 3/MA, 5B/DG) as well as NS2-Ubi-NS3
356 (2/VD, 2/TV, 4A/A48-T, 5B/DG) (Fig. 5B). While electroporation of RNA CSFV NS2-
357 Ubi-NS3 (2/VD, 2/TV, 3/MA, 5B/DG) resulted, as expected, in efficient virion
358 production, electroporation of RNA CSFV NS2-Ubi-NS3 (2/VD, 2/TV, 4A/A48-T,
359 5B/DG) yielded negligible virus titers (Fig. 5C). This experiment demonstrated that
360 also in the context of CSFV NS2-Ubi-NS3 mutation 3/MA is essential and cannot be
361 functionally substituted by the selected NS4A mutation 4A/A48-T.
362 In a previous study it was shown for BVDV-1 that the NS4A mutations L45-A and
363 Y47-A can functionally substitute for exchange of NS3 amino acid 132 to alanine
364 (14). Therefore, we tested for a functional redundancy of mutation 3/MA and NS4A
365 mutations 4A/L45-A or 4A/Y47-A in the context of CSFV NS2-Ubi-NS3.
366 *In vitro* RNA transcripts of variants CSFV NS2-Ubi-NS3 (2/VD, 2/TV, 4A/L45-A,
367 5B/DG) and CSFV NS2-Ubi-NS3 (2/VD, 2/TV, 4A/Y47-A, 5B/DG) were
368 electroporated into SK6 cells followed by titer analysis at 48 h pe and 72 h pi (MOI
369 0.1) (Fig. 5C). Efficient NS2-3-independent virion formation was observed for both
370 CSFV NS2-Ubi-NS3 derivatives with viral titers of about 2.6-3.5 x 10^6 $TCID_{50}$/ml (48 h
371 pe) and 4.6-6.3 x 10^7 $TCID_{50}$/ml (72 h pi MOI 0.1) (Fig. 5C). As expected, CSFV

NS2-Ubi-NS3 (2/VD, 2/TV, 5B/DG) did not produce infectious progeny. According to those results, NS4A mutations L45-A and Y47-A can indeed functionally substitute for mutation 3/MA in CSFV NS2-Ubi-NS3 (Fig. 5C). In conclusion, these experiments demonstrate that in the CSFV system, analogous to previous findings for BVDV-1, an alanine exchange at NS3 position 132 can be functionally mimicked by NS4A mutations L45-A or Y47-A. However, NS4A mutation A48-T does not have this capacity. The latter finding indicates that the NS4A mutation at position 48 selected in the context of CSFV NS2-IRES-$NS3_{SC}$ does not function as an effective modulator of the NS3/4A-kink interaction, in contrast to 3/MA, 4A/L45-A or 4A/Y47-A.

In summary, the studies on BVDV-1 and CSFV both demonstrate that the fine-tuning of the surface interaction between NS3 and the NS4A kink region is critical for switching the function of the NS3/4A complex between RNA replication and virion morphogenesis. This represents an elegant solution for using the same protein complex as a basic building block in two different steps in the viral life-cycle which endowes those viruses with an increased functional capacity of their very limited protein arsenals.

389

390 **Discussion**

391 Based on the finding that HCV does in contrast to BVDV-1 and CSFV not depend on
392 uncleaved NS2-3 for virion morphogenesis a selection approach was used to adapt
393 BVDV-1 strain NCP7 to virion assembly in the absence of uncleaved NS2-3. Based
394 on the identified gain-of-function mutations and the crystal structure of a single- chain
395 NS3-4A protease a crucial role of the NS3 surface interaction with the NS4A kink
396 region could be demonstrated for the switch between RNA replication and virion
397 morphogenesis: A compact conformation with a tightly bound NS4A kink region
398 supports RNA replicase formation while a more open NS3/4A complex with a less
399 stringent interaction between the NS4A kink region and the NS3 surface facilitates
400 virion morphogenesis but interferes with RNA replication. NS3 amino acid 132, which
401 is critical for the interaction with the NS4A kink region, plays a pivotal role in this
402 switch (14). In the present study an essential role of NS3 amino acid 132 in
403 modulating the switch between RNA replication and virion morphogenesis was also
404 verified for CSFV. Also in this pestivirus species the stimulating effect of the 3/M132-
405 A exchange for the NS2-3-independent virion morphogenesis is most likely based on
406 a weakening of surface interactions in the NS3/4A complex. This assumption is
407 based on the available crystal structure and is further corroborated by the
408 experimental data demonstrating that NS4A mutations L45-A and Y47-A in the CSFV
409 system were able to functionally substitute for the NS3 M132-A exchange (Fig. 5C).
410 Interestingly, this was not the case for the NS4A mutation A48-T which was selected
411 in the context of CSFV NS2-IRES-NS3 (Fig. 5C). The latter mutation was not able to
412 functionally rescue virion morphogenesis in CSFV NS2-Ubi-NS3 not carrying
413 mutation M132-A. This data correlates with observations derived from the crystal

structure of the NS3-4A single chain protease: While NS4A amino acids 45 and 47 undergo interactions with the NS3 surface surrounding M132 (14), the side chain of NS4A residue A48 does not (Fig. 5A). This supports the conclusion, that the supportive effect of the NS4A A48-T mutation on virion morphogenesis in the bicistronic context CSFV NS2-IRES-NS3 has a different mechanistic basis compared to the one of NS4A L45-A or Y47-A. Together, these observations clearly show that NS4A has regulatory role(s) in pestiviral virion morphogenesis (14).

In the absence of structural information no detailed role could be assigned to the mutation located in the C-terminal protease domain of NS2 (T444-V), an amino acid position which was also proven critical for virion formation in BVDV-1 NS2-Ubi-NS3. In this study we observed that for virion morphogenesis of CSFV NS2-Ubi-NS3 a second mutation in NS2 (V439-D) is absolutely required in addition to mutations NS2 T444-V and M132-A in NS3 (Fig. 4B). Since both mutations are only five amino acids apart from each other both may cooperate in their positive effect on NS2-3-independent virion formation. Since NS2 and NS3 have been artificially separated in the virus mutants used for selection it seems reasonable to assume that the mutations identified in NS2 may facilitate alternative NS2/NS3 interactions. Such NS2/NS3 interactions with a central role in coordinating virion morphogenesis have been described for HCV (24-28).

The bicistronic CSFV NS2-IRES-NS3 genome requires accessory mutations outside of the NS2-3 region for efficient virion morphogenesis in the absence of uncleaved NS2-3, an observation that is similar to what has been seen for BVDV-1 NS2-IRES-NS3 (23). In both virus species a mutation in NS5B (E145-G in BVDV-1 and D280-G in CSFV) turned out as beneficial for this phenotype (Fig. 2B and 2C) (23). Strikingly, in both cases an acidic amino acid residing in the first of the two finger domains (residues 136 to 313) of NS5B is replaced by a glycine residue (29). As described by

Li *et al.* the N-terminal part of the finger domain (residues 136 to 160), along with an insertion in the β-finger domain (residues 260 to 288), forms a fingertip region that bridges the finger and thumb domain. Accordingly, the NS5B mutations selected in BVDV-1 and CSFV reside exactly in those two amino acid stretches. In the structure published by Li *et al.* amino acids 145 and 280 are both located on a charged surface area of NS5B which also comprises a conserved basic residue at position 149 (R or K) and the highly conserved residues E151 and K152 (29). Of note, the cytopathogenic BVDV strain Osloss which encodes a ubiquitin monomer between NS2 and NS3 due to a natural recombination event also encodes a glycine residue at NS5B position 145 similar to what has been selected for NCP7 NS2-IRES-NS3 (23) and CSFV strains Alfort/Tuebingen and Alfort/187 both encode an alanine at NS5B position 145. These observations may indicate that a reduction of the surface charge in this region is promoting interaction(s) required for NS2-3-independent virion morphogenesis. Interestingly, the fingertip region has been implicated in interacting with the RNA template in BVDV NS5B (30, 31). This data supports the attractive working hypothesis, that the selected NS5B mutations alter the NS5B/genome interaction in a way which facilitates the formation of infectious virus particles around the newly synthetized genomes, by e.g. a more efficient transfer of the RNA to other viral RNA-binding proteins, e.g. NS5A, the NS3/4A complex or core. Alternatively or in addition, the positive effect observed for the so far selected loss of charge mutations at the NS5B surface may be based on a support of novel hydrophobic protein/protein interactions required for virion formation. One attractive binding partner for such an interaction could be NS4A since the NS4A mutation A48-T was co-selected with NS5B D280-G (Fig. 2B). For HCV an individual interaction between NS5B, NS3 and NS4A has been described (32). A functional role in HCV virion

morphogenesis has been assigned to NS4A in several studies (33, 34) and recently more specifically to a tyrosine residue at position 45 in the C-terminal domain (35). A potential effect of the NS5B mutation as well as for mutations NS4A A48-T and NS3 M132-A on polyprotein processing and RNA replication was analyzed using a bicistronic reporter replicon. At least with the assays applied, no or in case of the NS4A A48-T mutation, a minor negative effect on RNA replication was observed, similar to the results obtained for the compensatory mutations of BVDV-1 (23). With respect to the result obtained for NS5B mutation D280-G selected in this study it is remarkable that a previous report demonstrated that the region right downstream of D280 is highly critical for RNA polymerase activity (29). Thus, this set of mutations identified by *in vivo* selection is specifically capable of promoting virion assembly without diminishing the efficacy of RNA replication. These mutations as well as the mutations in NS2 may be relevant to establish or enhance protein/protein interactions required for virion morphogenesis, while mutations at position 132 in NS3 are required to open up the NS3/4A complex at the NS3/4A kink interaction surface. Further detailed studies aiming at changes in the viral interactome induced by the two independent sets of gain-of-function mutations described now for the pestivirus species BVDV-1 and CSFV are now possible and will facilitate the gain of a detailed understanding of the processes involved in pestiviral virion morphogenesis.

Journal of Virology

485 **Materials and Methods**

486 **Antibodies.** CSFV NS3/NS2-3 were detected with monoclonal antibody (Mab) C16
487 (36, 37). The antibodies for the detection of NS4A (GH4A1), NS4B (GL4B1), NS5A
488 (GL5A1) and NS5B (GR5B1) were kindly provided by T. Rümenapf (University of
489 Veterinary Medicine, Vienna, Austria) and B. Lamp (Justus-Liebig University
490 Giessen, Germany) (38). Mouse-specific cyanogen-3-labeled (Cy3) or peroxidase-
491 coupled (PO) antibodies were obtained from Dianova (Hamburg, Germany). The
492 antibody C4 directed against β–Actin was obtained from Santa Cruz Biotechnology,
493 Inc (Dallas, USA).
494
495 **Cells and viruses.** Swine kidney cells (SK6) (39), kindly provided by J. D. Tratschin
496 (Institute of Virology and Immunoprophylaxis, Mittelhäusern, Switzerland), were
497 cultivated in minimal essential medium (MEM) supplemented with 10% fetal calf
498 serum (FCS) (Thermo Fisher Scientific GmbH, Schwerte, Germany), 100 U/ml
499 penicillin and 100 µg/ml streptomycin. Huh7-T7 cells (40) were kept in Dulbecco's
500 modified Eagle's medium (DMEM) containing 10% FCS, 100 U/ml penicillin, 100
501 µg/ml streptomycin and 125 µg/ml G418 (Thermo Fisher Scientific GmbH, Schwerte,
502 Germany). All cells were cultivated at 37°C and 5% CO_2. The CSFV strain
503 Alfort/Tuebingen has been described previously (41). Modified-Vaccinia-Virus-Ankara
504 (MVA)-T7^{pol} was generously provided by G. Sutter (LMU, Munich, Germany) (42).
505
506 **Plasmid constructs.** Plasmids were generated by standard cloning techniques.
507 Mutations were introduced by PCR or site-directed mutagenesis (QuikChange^{TM},
508 Thermo Fisher Scientific GmbH, Schwerte, Germany). All constructs were verified by
509 restriction enzyme digestion and sequencing. PCR products were subcloned using
510 the pGEM-T Vector System I (Promega, Madison, WI, USA). All amino acid numbers

refer to the individual sequence of the respective protein encoded by CSFV Alfort/Tuebingen (accession number: J04358.2). Underlined sequences of PCR primers highlight recognition sites of restriction enzymes which were used for cloning.

CSFV full length constructs and subclones. CSFV full length constructs are based on the previously described cDNA clone p447 of CSFV strain Alfort/Tuebingen (41). The vectors LITMUS 28i and LITMUS 38i were obtained from New England Biolabs (NEB, Ipswich, MA, USA). LITMUS 28i was cleaved with the restriction enzymes *EcoRV* and *DraIII* and the 1.2-kb fragment was ligated into the 1.6-kb vector fragment of LITMUS 38i generated by EcoRV/DraIII-restriction resulting in plit28/38. The plasmid plit28/38 CSFV NsiI-NS5B-3'UTR-BamHI was generated by ligation of the NsiI/BamHI-fragment of p447 into the vector fragment of plit28/38 cleaved with *NsiI* and *BamHI* restriction enzymes. The subclone plit28/38 CSFV NsiI-NS5B-3'UTR-BamHI was used as template for QuikChange™ PCR with the primers CSFV NS5B/GAA se (5'-gcaaagatccatgtctgcggggcggccggcttcctgattaccgaaag-3') and CSFV NS5B/GAA ase (5'-ctttcggtaatcaggaagccggccgccccgcagacatggatctttgc-3') to introduce alanine mutations at NS5B positions D448 and D449 (5B/GAA) to inactivate the viral RNA-dependent RNA polymerase NS5B generating plit28/38 CSFV NsiI-NS5B-3'UTR-BamHI (5B/GAA). To generate full length pCSFV (5B/GAA) the NsiI/BamHI-fragment of plit28/38 CSFV NsiI-NS5B-3'UTR-BamHI (5B/GAA) was cloned into the p447 vector fragment cleaved with *NsiI* and *BamHI*.

The plasmid pCITE-2a containing the internal ribosomal entry site (IRES) of encephalomyocarditis virus (EMCV) downstream of the T7 RNA polymerase promotor was obtained from Novagen (Madison, WI, USA). To generate full length pCSFV NS2-IRES-NS3, the C-terminal part of NS2 was amplified by PCR from p447 template using the primers CSFV NS2 se (5'-agatctagtcatagccacag-3') and CSFV NS2 ase (5'-acgcgtctatctaagcacccagccaaggtg-3') and were subcloned into pGEM-T

resulting in pGEM-T CSFV BglII-NS2-Stopp-MluI. This subclone was used as template DNA for site-directed mutagenesis with the primers NS2(ΔC) se (5'-cgttttggaccaccagtggtcggtatgaccctagccgatttcg-3') and NS2(ΔC) ase (5'-cgaaatcggctagggtcataccgaccactggtggtccaaaacg-3') to delete the active site cysteine of the NS2 protease (ΔC380, deletion of NS2 amino acid C380) resulting in pGEM-T CSFV BglII-NS2-Stopp-MluI (ΔC380). The EMCV-IRES was amplified from pCITE-2a with the primers EMCV-IRES se (5'- acgcgtccggttattttccaccatattgc-3') and EMCV-IRES ase (5'- ccatggtattatcatcgtgtttt-3') resulting in pGEM-T MluI-IRES-NcoI. In addition, the N-terminal part of CSFV NS3 was amplified from p447 using the primers CSFV NS3 se (5'-ccatggggccagctgtttgcaagaagg-3') and CSFV NS3 ase (5'-gaattctccacccgttttctgtaag-3') and the PCR fragment was subcloned into pGEM-T resulting in pGEM-T CSFV NcoI-NS3-EcoRI. The fragments BglII-NS2-Stopp-MluI (ΔC), MluI-IRES-NcoI and NcoI-NS3-EcoRI were obtained from the respective pGEM-T subclones by restriction with the indicated flanking restriction enzymes and cloned into the p447 vector fragment which was generated by BglII/EcoRI-restriction resulting in pCSFV NS2-IRES-NS3.

The subclone plit28/38 CSFV BglII-NS2-IRES-NS3-EcoRI was generated by ligation of the BglII/EcoRI-fragment of pCSFV NS2-IRES-NS3 into the vector fragment of plit28/38 generated by cleavage with *BglII* and *EcoRI* restriction sites. In addition, the EcoRI/NgoMIV-fragment of p447 was subcloned into the plit38 vector which was cleaved with *EcoRI* and *NgoMIV* resulting in plit38 CSFV EcoRI-NS3-NS4A-NS4B-NgoMIV. Also, the SbfI/BglII-fragment of p447 was ligated with the respective vector fragment of plit28/38 resulting in plit28/38 CSFV SbfI-E^{rns}-E1-E2-NS2-BglII.

The construct pUb 1590-5B has been described earlier (43). Full length construct pCSFV NS2-Ubi-NS3 was generated as follows: the C-terminal part of NS2 was amplified by PCR from template pCSFV NS2-IRES-NS3 using primers CSFV NS2 se

(5'-agatctagtcatagccacag-3') and CSFV NS2-BspMI ase (5'-acctgcatttgcattctaagcacccagccaagg -3') and the PCR product was cloned into pGEM-T vector resulting in pGEM-T CSFV BglII-NS2(ΔC)-BspMI. Murine ubiquitin (Ubi) was amplified by PCR from pUb 1590-5B with the primers BsmBI-Ubi(ΔBglII) se (5'-cgtctccatgcaaatcttcgtgaaaaccctgacg-3') and Ubi-BsmBI ase (5'-cgtctcctcctccgcggagtcgcagcaccaggtgcaagg-3') and subcloned into pGEM-T resulting in pGEM-T BsmBI-Ubi(ΔBglII)-BsmBI. In addition, the N-terminal part of NS3 was amplified by PCR from template p447 using PCR primers CSFV SacII-NS3 se (5-ccgcggaggagggccagctgtttgcaagaagg-3) and CSFV NS3 ase (5'-gaattctccacccgttttctgtaag-3') and ligated into pGEM-T resulting in pGEM-T CSFV SacII-NS3-EcoRI. Subsequently, the fragments BglII-NS2(ΔC)-BspMI, BsmBI-Ubi(ΔBglII)-BsmBI, SacII-NS3-EcoRI were ligated into the plit28 vector cleaved with BglII and EcoRI resulting in plit28 CSFV BglII-NS2-Ubi-NS3-EcoRI. To generate pCSFV NS2-Ubi-NS3 the BglII/EcoRI-fragment was obtained from plit28 CSFV BglII-NS2-Ubi-NS3-EcoRI and ligated into the p447 vector cleaved with *BglII/EcoRI*.

The mutations E1/A83-T, 2/Q147-K, 2/V439-D, 2/T444-V, 3/M132-A, 3/L385-I, 4A/L45-A, 4A/Y47-A, 4A/A48-T and 5B/D280-G were introduced by QuikChange™-PCR with appropriate primer pairs (detailed sequences can be obtained upon request) into respective subclones which are given above. Subsequently, mutations were reintroduced into pCSFV NS2-IRES-NS3 or pCSFV NS2-Ubi-NS3 by ligation of respective DNA-fragments generated with the restriction enzymes indicated above.

CSFV bicistronic reporter replicon. The BVDV bicistronic reporter replicon pBici RLuc IRES-Ubi-NS3-3' has been described (14). The SP6 promotor sequence, the CSFV 5'UTR and N^{pro} was amplified from p447 template by PCR using primers CSFV 5'UTR-Npro se (5'-tctagaatttaggtgacactatagtatacg-3') and CSFV Npro ase (5'-gcgcgcaactggttacccataatgg-3') and ligated into pGEM-T vector resulting pGEM-T

589 XbaI-SP6-CSFV 5'UTR-Npro-BssHII. The chimeric pBici/CSFV 5'UTR Npro RLuc
590 IRES-Ubi-NS3-3' was generated by ligating XbaI-SP6-CSFV 5'UTR-Npro-BssHII into
591 the vector fragment of pBici RLuc IRES-Ubi-NS3-3' cleaved with *NheI* and *BssHII*.
592 Subsequently, the 866-bp NotI/SacII-fragment of pBici/CSFV 5'UTR Npro RLuc
593 IRES-Ubi-NS3-3' and the 7.162-bp SacII/SmaI-fragment of p447 were ligated into the
594 pBici/CSFV 5'UTR Npro RLuc IRES-Ubi-NS3-3' vector cleaved with *SmaI* and *NotI*
595 generating pCSFV Bici RLuc IRES-Ubi-NS3-3'. Variants of pCSFV Bici RLuc IRES-
596 Ubi-NS3-3' encoding the mutations 3/M132-A, 4A/A48-T and 5B/D280-G were
597 generated using respective subclones and restriction enzymes indicated above.
598
599 ***In vitro* transcription and RNA electroporation.** Electroporation of CSFV full length
600 or replicon RNAs into SK6 cells was carried out as it has been described previously
601 for the electroporation of BVDV RNAs into MDBK cells (44). Briefly, 2 µg of plasmid
602 DNA were linearized with *SmaI* (NEB, Ipswich, MA, USA) and used as template for *in*
603 *vitro* transcription with MAXIscript SP6 transcription kit (Ambion, Thermo Fisher
604 Scientific GmbH, Schwerte, Germany) according to manufacturer's instructions.
605 Subsequently, 1 µg RNA was used for the electroporation of 3 x 10^6 SK6 cells
606 (conditions: 180 V, 950 µF, 2 mm gap cuvette). After electroporation, cells were
607 immediately resuspended in complete MEM and seeded as required into 6-well
608 plates. At the indicated time points post electroporation (pe), cell culture supernatants
609 were harvested and passed thorough a 0,22 µm filter and cells were processed for
610 *Renilla* luciferase assay or immunofluorescence assay, respectively.
611
612 **DNA transfection and transient protein expression.** Huh7-T7 cells (40) were
613 infected with modified vaccinia virus Ankara-$T7^{pol}$ (MVA-$T7^{pol}$) (42) for 1 h at 37°C.
614 Subsequently, cells were transfected with 6 µg of plasmid DNA using

polyethylenimine (PEI) as transfection reagent according to manufacturer's protocol (Polysciences, Inc., Warrington, PA, USA). Expression was carried out for 18 h at 37°C.

SDS-PAGE and Western blotting. The cells of one 6-well were lysed in 120 µl SDS-sample buffer and boiled for 10 min at 95°C. Subsequently, 20 µl of cell lysate were separated with SDS-polyacrylamide-Tricine gels (8 or 10% polyacrylamide) (45). After electrophoresis, proteins were transferred onto nitrocellulose membranes (Pall, Pensacola, FL, USA). Membranes were blocked with 5% (wt/vol) skim milk powder (Roth, Karlsruhe, Germany) in PBS with 0.05% (vol/vol) Tween 20 (Thermo Fisher Scientific GmbH, Schwerte, Germany). CSFV proteins were detected with the indicated monoclonal antibodies and visualized with mouse-specific peroxidase-coupled secondary antibody. The Western Lightning chemiluminescence reagent (PerkinElmer, Boston, MA, USA) was applied.

Luciferase assay. Bicistronic reporter constructs, encoding CSFV N^{pro} and *Renilla* luciferase in the first ORF and one monomer of ubiquitin followed by CSFV NS3-5B in the second ORF, were used to determine RNA replication efficiencies as it has been described (4). The *Renilla* Glow-Juice Luciferase Assay (PJK, Kleinblittersdorf, Germany) was used according to manufacturer's instructions. Briefly, cells were harvested at the indicated time points (2 h, 24 h, 48 h pe) and stored at -80°C. Subsequently, cells were lysed in 40 µl lysis juice and 20 µl of the cell lysates were mixed with 100 µl of *Renilla* Glow juice containing 2 µl of substrate solution. Luciferase activities were determined as relative light units (RLUs) with a Junior LB 9509 portable Tube Luminometer (Junior LB9509, Berthold, Bad Wildbad, Germany).

641 **CSFV infection and virus titration.** Cell culture supernatants of SK6 cells were
642 harvested at indicated time points post electroporation (pe) or post infection (pi) and
643 passed through a 0.22-µm cellulose filter (Sartorius, Goettingen, Germany).
644 Infection of 4 x 10^5 SK6 cells with multiplicity of infection (MOI) 0.1 was performed for
645 1 h at 37°C in MEM containing all supplements. Afterwards, cells were washed three
646 times with PBS and cultivated in 2 ml of MEM containing all supplements.
647 Viral titers of cell culture supernatants were determined by endpoint titration as tissue
648 culture infection dose 50 per ml ($TCID_{50}$/ml). Titration was performed in four
649 replicates using SK6 cells. Viral infection was detected 72 h pi by IF with C16 (36,
650 37) directed against NS3/NS2-3. Mouse-specific Cy3-labeled secondary antibody
651 (Dianova, Hamburg, Germany) was used at dilution 1:2.000.
652
653 **Virus plaque purification.** SK6 cells were seeded into 6-well plates and infections
654 with different dilutions of cell culture supernatants containing infectious CSFV were
655 performed. 1 h post infection, cells were washed three times with PBS and cells were
656 overlaid with MEM containing all supplements and 0.6% low-melting-point agarose
657 (Roth, Karlsruhe, Germany). Individual CSFV-specific plaques became visible after
658 72-96 h pi, due to the cytopathic effect, and were isolated using a 1000 µl pipette tip.
659 After three consecutive rounds of plaque purification individual virus clones were
660 used to infect naïve SK6 cells followed by viral RNA isolation and sequence
661 determination.
662
663 **RNA isolation, reverse transcription-PCR (RT-PCR), and direct sequencing of**
664 **viral genomes.** Viral RNA was isolated from cell culture supernatants of CSFV
665 infected SK6 cells containing infectious CSFV using the QIAamp Viral RNA Mini Kit
666 (Qiagen, Hilden, Germany) according to manufacturer's instructions. cDNA

fragments were generated by using Superscript II Reverse Transcriptase (Thermo Fisher Scientific GmbH, Schwerte, Germany) followed by amplification with the Expand Long Template PCR System (Roche, Mannheim, Germany). Primer sequences can be obtained upon request. The amplicons were purified by agarose gel electrophoresis followed by gel elution with QIAquick Gel Extraction Kit (Qiagen, Hilden, Germany). Subsequently, the purified PCR fragments were directly sequenced using appropriate primers.

Nucleotide sequencing. DNA sequencing was performed at LGC Sequencing Services (LGC Genomics GmbH, Berlin, Germany). Sequences were further analyzed using the Vector NTI software (Thermo Fisher Scientific GmbH, Schwerte, Germany).

Immunofluorescence analysis. Detection of CSFV-positive cells was performed at the indicated time points by indirect immunofluorescence analysis (IF). For this, cells were washed with PBS and fixed with 2% (wt/vol) paraformaldehyde (Thermo Fisher Scientific GmbH, Schwerte, Germany) in PBS for 20 min at 4°C. Permeabilization was achieved by incubation with 0.5% (wt/vol) N-octyl-β-D-glycopyranoside (Sigma-Aldrich Chemie GmbH, Taufkirchen, Germany) in PBS for 10 min at 4°C. Cells were washed with PBS and incubated for 20 min at 37°C with blocking solution containing 2% (wt/vol) bovine serum albumin (BSA, Carl Roth GmbH + Co. KG, Karlsruhe, Germany) in PBS with 0.05% (vol/vol) Tween 20 (Thermo Fisher Scientific GmbH, Schwerte, Germany) (PBS-T). Detection of NS3/NS2-3 was performed with mAb C16 (36, 37) in a dilution of 1:100 in blocking solution. After 1h, cells were washed with blocking solution and incubated with mouse-specific Cy3-labeled secondary antibody (Dianova, Hamburg, Germany) in a dilution of 1:2.000 in blocking solution for 1 h at

37°C. In parallel, cellular nuclei were stained with DAPI. Subsequently, cells were washed with PBS-T and images were obtained with a Zeiss Axio Observer.Z1 fluorescence microscope (Zeiss, Göttingen,Germany).

Acknowledgements

We are grateful to E. J. Dubovi (Cornell University, Ithaca, NY) for antibody 8.12.7, T. Rümenapf (University of Veterinary Medicine, Vienna, Austria) and B. Lamp (Justus-Liebig University Giessen, Germany) for providing antibodies GH4A1, GL4B1, GL5A1 and GR5B1, S. Lemon (UNC, Chapel Hill, NC) for providing us with the Huh7-T7 cell line, and G. Sutter (LMU, Munich, Germany) for the MVA-T7^{pol} vaccinia virus. We especially thank O. Isken and all members of the Tautz group for support and critical reading of the manuscript. We also thank Kyung Choi (The University of Texas Medical Branch) for helpful discussions.

Authors made the following contributions: conceived and designed the experiments, D.D., and N.T.; generated reagents, O.K.; performed the experiments, D.D., S.S., and H.B.; analyzed the data, D.D., H.B., and N.T.; wrote the paper, D.D. and N.T.

References

1. **Simmonds P, Becher P, Bukh J, Gould EA, Meyers G, Monath T, Muerhoff S, Pletnev A, Rico-Hesse R, Smith DB, Stapleton JT, Ictv Report C.** 2017. ICTV Virus Taxonomy Profile: Flaviviridae. J Gen Virol **98:**2-3.
2. **Tautz N, Tews BA, Meyers G.** 2015. The Molecular Biology of Pestiviruses. Adv Virus Res **93:**47-160.
3. **Murray CL, Jones CT, Rice CM.** 2008. Architects of assembly: roles of Flaviviridae non-structural proteins in virion morphogenesis. Nat Rev Microbiol **6:**699-708.
4. **Isken O, Langerwisch U, Schonherr R, Lamp B, Schroder K, Duden R, Rumenapf TH, Tautz N.** 2014. Functional characterization of bovine viral diarrhea virus nonstructural protein 5A by reverse genetic analysis and live cell imaging. J Virol **88:**82-98.
5. **Agapov EV, Murray CL, Frolov I, Qu L, Myers TM, Rice CM.** 2004. Uncleaved NS2-3 Is Required for Production of Infectious Bovine Viral Diarrhea Virus. J Virol **78:**2414-2425.
6. **Moulin HR, Seuberlich T, Bauhofer O, Bennett LC, Tratschin JD, Hofmann MA, Ruggli N.** 2007. Nonstructural proteins NS2-3 and NS4A of classical swine fever virus: essential features for infectious particle formation. Virology **365:**376-389.
7. **Ansari IH, Chen LM, Liang D, Gil LH, Zhong W, Donis RO.** 2004. Involvement of a bovine viral diarrhea virus NS5B locus in virion assembly. J Virol **78:**9612-9623.
8. **Harada T, Tautz N, Thiel H-J.** 2000. E2-p7 region of the bovine viral diarrhea virus polyprotein: processing and functional studies. J Virol **74:**9498-9506.
9. **Liang D, Chen L, Ansari IH, Gil LH, Topliff CL, Kelling CL, Donis RO.** 2009. A replicon trans-packaging system reveals the requirement of nonstructural proteins for the assembly of bovine viral diarrhea virus (BVDV) virion. Virology **387:**331-340.
10. **Han Q, Manna D, Belton K, Cole R, Konan KV.** 2013. Modulation of hepatitis C virus genome encapsidation by nonstructural protein 4B. J Virol **87:**7409-7422.
11. **Paul D, Romero-Brey I, Gouttenoire J, Stoitsova S, Krijnse-Locker J, Moradpour D, Bartenschlager R.** 2011. NS4B self-interaction through conserved C-terminal elements is required for the establishment of functional hepatitis C virus replication complexes. J Virol **85:**6963-6976.
12. **Tamura JK, Warrener P, Collett MS.** 1993. RNA-stimulated NTPase activity associated with the p80 protein of the pestivirus bovine viral diarrhea virus. Virology **193:**1-10.
13. **Warrener P, Collett MS.** 1995. Pestivirus NS3 (p80) protein possesses RNA helicase activity. J Virol **69:**1720-1726.
14. **Dubrau D, Tortorici MA, Rey FA, Tautz N.** 2017. A positive-strand RNA virus uses alternative protein-protein interactions within a viral protease/cofactor complex to switch between RNA replication and virion morphogenesis. PLoS Pathog **13:**e1006134.
15. **Lackner T, Müller A, König M, Thiel H-J, Tautz N.** 2005. Persistence of bovine viral diarrhea virus is determined by a cellular cofactor of a viral autoprotease. J Virol **79:**9746-9755.

16. **Grassmann CW, Isken O, Behrens SE.** 1999. Assignment of the Multifunctional NS3 Protein of Bovine Viral Diarrhea Virus during RNA Replication: an In Vivo and In Vitro Study. J Virol **73:**9196-9205.
17. **Rinck G, Birghan C, Harada T, Meyers G, Thiel H-J, Tautz N.** 2001. A cellular J-domain protein modulates polyprotein processing and cytopathogenicity of a pestivirus. J Virol **75:**9470-9482.
18. **Isken O, Postel A, Bruhn B, Lattwein E, Becher P, Tautz N.** 2018. CRISPR/Cas9-mediated knock-out of DNAJC14 verifies this chaperone as a pivotal host factor for RNA replication of Pestiviruses. J Virol doi:10.1128/JVI.01714-18.
19. **Jones CT, Murray CL, Eastman DK, Tassello J, Rice CM.** 2007. Hepatitis C virus p7 and NS2 proteins are essential for production of infectious virus. J Virol **81:**8374-8383.
20. **Jirasko V, Montserret R, Appel N, Janvier A, Eustachi L, Brohm C, Steinmann E, Pietschmann T, Penin F, Bartenschlager R.** 2008. Structural and functional characterization of nonstructural protein 2 for its role in hepatitis C virus assembly. J Biol Chem **283:**28546-28562.
21. **Lattwein E, Klemens O, Schwindt S, Becher P, Tautz N.** 2012. Pestivirus virion morphogenesis in the absence of uncleaved nonstructural protein 2-3. J Virol **86:**427-437.
22. **Meyers G, Rümenapf T, Thiel H-J.** 1989. Ubiquitin in a togavirus. Nature **341:**491.
23. **Klemens O, Dubrau D, Tautz N.** 2015. Characterization of the Determinants of NS2-3-Independent Virion Morphogenesis of Pestiviruses. J Virol **89:**11668-11680.
24. **Jones DM, Atoom AM, Zhang X, Kottilil S, Russell RS.** 2011. A genetic interaction between the core and NS3 proteins of hepatitis C virus is essential for production of infectious virus. J Virol **85:**12351-12361.
25. **Popescu CI, Callens N, Trinel D, Roingeard P, Moradpour D, Descamps V, Duverlie G, Penin F, Heliot L, Rouille Y, Dubuisson J.** 2011. NS2 Protein of Hepatitis C Virus Interacts with Structural and Non-Structural Proteins towards Virus Assembly. PLoS Pathog **7:**e1001278.
26. **Stapleford KA, Lindenbach BD.** 2011. Hepatitis C virus NS2 coordinates virus particle assembly through physical interactions with the E1-E2 glycoprotein and NS3-NS4A enzyme complexes. J Virol **85:**1706-1717.
27. **Ma Y, Anantpadma M, Timpe JM, Shanmugam S, Singh SM, Lemon SM, Yi M.** 2011. Hepatitis C virus NS2 protein serves as a scaffold for virus assembly by interacting with both structural and nonstructural proteins. J Virol **85:**86-97.
28. **Boson B, Granio O, Bartenschlager R, Cosset FL.** 2011. A concerted action of hepatitis C virus p7 and nonstructural protein 2 regulates core localization at the endoplasmic reticulum and virus assembly. PLoS Pathog **7:**e1002144.
29. **Li W, Wu B, Soca WA, An L.** 2018. Crystal Structure of Classical Swine Fever Virus NS5B Reveals a Novel N-Terminal Domain. J Virol **92**.
30. **Choi KH, Groarke JM, Young DC, Kuhn RJ, Smith JL, Pevear DC, Rossmann MG.** 2004. The structure of the RNA-dependent RNA polymerase from bovine viral diarrhea virus establishes the role of GTP in de novo initiation. Proc Natl Acad Sci U S A **101:**4425-4430.

31. **Choi KH, Gallei A, Becher P, Rossmann MG.** 2006. The structure of bovine viral diarrhea virus RNA-dependent RNA polymerase and its amino-terminal domain. Structure **14:**1107-1113.
32. **Ishido S, Fujita T, Hotta H.** 1998. Complex formation of NS5B with NS3 and NS4A proteins of hepatitis C virus. Biochem Biophys Res Commun **244:**35-40.
33. **Phan T, Kohlway A, Dimberu P, Pyle AM, Lindenbach BD.** 2011. The acidic domain of hepatitis C virus NS4A contributes to RNA replication and virus particle assembly. J Virol **85:**1193-1204.
34. **Kohlway A, Pirakitikulr N, Barrera FN, Potapova O, Engelman DM, Pyle AM, Lindenbach BD.** 2014. Hepatitis C virus RNA replication and virus particle assembly require specific dimerization of the NS4A protein transmembrane domain. J Virol **88:**628-642.
35. **Roder AE, Vazquez C, Horner SM.** 2019. The acidic domain of the hepatitis C virus NS4A protein is required for viral assembly and envelopment through interactions with the viral E1 glycoprotein. PLoS Pathog **15:**e1007163.
36. **Peters W, Greiser-Wilke I, Moennig V, Liess B.** 1986. Preliminary serological characterization of bovine viral diarrhoea virus strains using monoclonal antibodies. Vet Microbiol **12:**195-200.
37. **Greiser-Wilke I, Dittmar KE, Liess B, Moennig V.** 1992. Heterogeneous expression of the non-structural protein p80/p125 in cells infected with different pestiviruses. J Gen Virol **73:**47-52.
38. **Lamp B, Riedel C, Roman-Sosa G, Heimann M, Jacobi S, Becher P, Thiel H-J, Rümenapf T.** 2011. Biosynthesis of Classical swine fever virus nonstructural proteins. J Virol **85:**3607-3620.
39. **Kasza L, Shadduck JA, Christofinis GJ.** 1972. Establishment, viral susceptibility and biological characteristics of a swine kidney cell line SK-6. Res Vet Sci **13:**46-51.
40. **Schultz DE, Honda M, Whetter LE, McKnight KL, Lemon SM.** 1996. Mutations within the 5' nontranslated RNA of cell culture-adapted hepatitis A virus which enhance cap-independent translation in cultured African green monkey kidney cells. J Virol **70:**1041-1049.
41. **Meyers G, Rümenapf T, Thiel H-J.** 1989. Molecular cloning and nucleotide sequence of the genome of hog cholera virus. Virology **171:**555-567.
42. **Sutter G, Ohlmann M, Erfle V.** 1995. Non-replicating vaccinia vector efficiently expresses bacteriophage T7 RNA polymerase. FEBS Letters **371:**9-12.
43. **Tautz N, Kaiser A, Thiel H-J.** 2000. NS3 serine protease of bovine viral diarrhea virus: characterization of active site residues, NS4A cofactor domain, and protease-cofactor interactions. Virology **273:**351-363.
44. **Tautz N, Harada T, Kaiser A, Rinck G, Behrens SE, Thiel H-J.** 1999. Establishment and characterization of cytopathogenic and noncytopathogenic pestivirus replicons. J Virol **73:**9422-9432.
45. **Schägger H, von Jagow G.** 1987. Tricine-sodium dodecyl sulfate-polyacrylamide gel electrophoresis for the separation of proteins in the range from 1 to 100 kDa. Anal Biochem **166:**368-379.

Figure Legends

FIG 1 The exchanges 2/TV and 3/MA enable low level CSFV formation in absence of NS2-3. (A) Schematic genome representation of the CSFV wild-type (WT) strain Alfort/Tuebingen. The derivative CSFV NS2-Ubi-NS3 (2/TV, 3/MA) encoding an ubiquitin gene (Ubi) between NS2 and NS3 as well as the bicistronic variant CSFV NS2-IRES-NS3 (2/TV, 3/MA) containing an EMCV-IRES between NS2 and NS3 are depicted. Amino acid substitutions T444-V in NS2 (2/TV) and M132-A in NS3 (3/MA) as well as the flanking 5'- and 3'-NTRs are indicated. (B) SK6 cells were electroporated with 1 µg of *in vitro* transcribed RNA of the indicated cDNA genomes. Top: RNA replication competence of the indicated full length RNAs was detected indirectly by NS3-specific immunofluorescence (IF) staining at 24 h post electroporation (pe). Nuclei were DAPI stained. Middle: At 48 h pe cell culture supernatants were harvested, and cells were analyzed by NS3-IF. Bottom: SK6 cells were inoculated with 500 µl of cell culture supernatants which were harvested at 48 h pe. At 72 h post infection (pi), CSFV-infected cells were detected by NS3-specific IF. (C) Viral titers of cell culture supernatants collected at 48 h pe were determined by endpoint titration as $TCID_{50}$/ml. Mean values and standard deviations of three experiments are depicted. Presence (+) or absence (-) of mutations 2/TV and 3/MA are indicated. 5B/GAA, RNA replication-deficient variant (negative control). (D) Western blot analyses of SK6 cells electroporated with genomic RNA transcripts and harvested 24 h pe. The RNAs used for electroporation are indicated above. The molecular weight is indicated on the left. For detection a NS3-specific monoclonal antibody was applied. β–Actin levels served as loading control and were detected by a respective monoclonal antibody.

878

879 **FIG 2 Serial cell culture passages of CSFV NS2-IRES-NS3 (2/TV, 3/MA) led to**
880 **the identification of titer enhancing mutations in NS2, NS4A and NS5B.** (A)
881 Schematic depiction of CSFV NS2-IRES-NS3 (2/TV, 3/MA) and flow chart of the
882 performed experiment. Serial cell culture passages followed by biological cloning (sc)
883 led to isolation of CSFV NS2-IRES-$NS3_{sc}$ encoding the additional mutations E1/A83-
884 T, 2/Q147-K, 2/V439-D, 3/L385-I, 4A/A48-T and 5B/D280-G. CSFV NS2-IRES-$NS3_{8-}$
885 $_{mut}$ contains 8 mutations derived from CSFV NS2-IRES-$NS3_{sc}$, i.e. E1/A83-T, 2/Q147-
886 K, 2/V439-D, 3/L385-I, 4A/A48-T and 5B/D280-G, as well as 2/TV, 3/MA. CSFV NS2-
887 IRES-$NS3_{5\text{-}mut}$ encompasses a minimal set of five mutations sufficient for high titer
888 virion morphogenesis, i.e. 2/V439-D, 2/T444-V, 3/M132-A, 4A/A48-T and 5B/D280-G.
889 (B) Experimental determination of a minimal set of mutations required for efficient
890 virion morphogenesis. Omitting each mutation individually from CSFV NS2-IRES-
891 $NS3_{8\text{-}mut}$ followed by determination of the titer at 48 h pe and 72 h pi (MOI 0.1 - if
892 possible) as $TCID_{50}$/ml revealed the five mutations 2/V439-D, 2/T444-V, 3/M132-A,
893 4A/A48-T and 5B/D280-G as critical for efficient NS2-3-independent virion formation.
894 Mean values and standard deviations of two independent experiments are depicted.
895 N.d.: not determined (the titer necessary for infection at MOI 0.1 was not achieved).
896 Statistical analyses of the titers obtained in the infection experiments using the
897 ANOVA test revealed no statistically significant differences between the titers of wt
898 and the individual mutant viruses. (C) Comparison of the selected biologically cloned
899 virus CSFV NS2-IRES-$NS3_{sc}$ with the respective viruses derived from cDNA clones
900 pCSFV NS2-IRES-$NS3_{8\text{-}mut}$ and pCSFV NS2-IRES-$NS3_{5\text{-}mut}$. SK6 cells were infected
901 with the indicated viruses at MOI 0.1. At 72 h pi cell culture supernatants were
902 harvested and virus titers were determined. Mean values and standard deviations of
903 four independent experiments are depicted. Statistical analyses of the titers obtained

in the infection experiments using Student's t-test are depicted in the graph (α = 0.05; * = $p < 0.05$; ns = not significant). CSFV WT, CSFV wild-type strain Alfort/Tuebingen (positive control).

FIG 3 The mutation 3/MA, 4A/A48-T and 5B/DG which are critical for efficient NS2-3-independent formation of CSFV neither affect polyprotein processing nor RNA replication. (A) Top: Scheme of the bicistronic reporter replicon CSFV Bici RLuc IRES-Ubi-NS3-3' coding for N^{pro} and *Renilla* luciferase in the first ORF while the viral replicase proteins NS3-5B are encoded in the second ORF. Ubiquitin (Ubi) was inserted upstream of NS3 to generate the authentic N terminus of NS3. Full length replicon RNA can be generated by *in vitro* transcription with SP6 RNA polymerase (SP6 promotor – grey arrow). Since a T7 promotor (black arrow) was inserted upstream of the second ORF, it can be transcribed (dashed line) using T7 RNA polymerase ($T7^{pol}$) to analyze polyprotein processing in a replication-independent manner. Bottom: Schematic drawing of the experimental setup. (B) Huh7-T7 cells were infected with Modified-Vaccinia-Virus-Ankara (MVA) encoding $T7^{pol}$ to increase $T7^{pol}$ amounts. 1 h post infection, cells were transfected with plasmid DNA of the indicated pCSFV Bici RLuc IRES-Ubi-NS3-3' variants followed by T7-mediated expression for 18 h. Subsequently, cells were lysed in sample buffer and protein samples were separated by SDS-PAGE followed by western blot analyses. Proteins were visualized using the indicated protein-specific primary antibodies. Mock, untransfected cells - negative control; 3/S163-A, inactivated NS3 protease - negative control for polyprotein processing; 5B/GAA, RNA replication-deficient mutant - negative control for RNA replication; WT, wild-type; the mutations 3/MA, 4A/A48-T and 5B/DG are indicated. Western blots of one representative experiment are depicted. Molecular mass markers are indicated in kilodaltons (kDa) on the left.

Protein products are depicted on the right. (C) Top: Scheme of CSFV RLuc IRES-Ubi-NS3-3' highlighting the SP6 RNA polymerase promotor and the respective RNA transcript (dashed line) that was used to generate full length replicon RNA. Bottom: Experimental setup to analyze RNA replication efficacies. (D) SK6 cells were electroporated with 1 µg of wild-type (WT) or the indicated mutated replicon RNAs. At given time points pe cells were harvested followed by lysis and determination of luciferase activities as relative light units (RLUs). Mean values and standard deviations of three experiments are depicted.

FIG 4 The mutation 2/VD promotes efficient formation of infectious CSFV NS2-Ubi-NS3 (2/TV, 3/MA). (A) Schematic representation of CSFV wild-type (WT) strain Alfort/Tuebingen and the derivative CSFV NS2-Ubi-$NS3_{5\text{-mut}}$ encoding an ubiquitin (Ubi) moiety between NS2 and NS3, thereby preventing formation of NS2-3. In addition, the bicistronic derivative CSFV NS2-IRES-$NS3_{5\text{-mut}}$ containing an EMCV-IRES between NS2 and NS3 is depicted. The five mutations (5-mut) 2/V439-D, 2/T444-V, 3/M132-A, 4A/A48-T and 5B/D280-G are indicated. (B) SK6 cells were electroporated with *in vitro* transcribed RNA of variants of CSFV NS2-Ubi-NS3 encoding the indicated mutations. 48 h pe viral supernatants were collected and analyzed for infectious virus by limited dilution assay as $TCID_{50}$/ml. In addition, infections at MOI 0.1 were performed and viral titers of supernatants collected at 72 h pi were determined. Mean values and standard deviations of three experiments are depicted. Statistical analyses of the titers obtained in the infection experiments using Student's t-test are depicted in the graph ($\alpha = 0.05$; * = $p < 0.05$; ** = $p < 0.01$). (C) Western blot analyses of SK6 cells electroporated with genomic RNA transcripts and harvested 24 h pe. The RNAs used for electroporation are indicated above. The molecular weight is indicated on the left. For detection a NS3-specific monoclonal

antibody was applied. β–Actin levels served as loading control and were detected by a respective monoclonal antibody. (D) Comparison of bicistronic derivatives CSFV NS2-IRES-NS3$_{5\text{-mut}}$ and CSFV NS2-IRES-NS3$_{3\text{-mut}}$ encoding the indicated mutations. Experiments were performed as described above; viral titers were determined at 48 h pe and 72 h pi (MOI 0.1). Mean values and standard deviations of two experiments are depicted. Presence (+) or absence (-) of the respective mutations are indicated. N.d., not determined.

FIG 5 The mutation 3/MA can be functionally substituted by single alanine exchanges at positions L45 and Y47 but not by mutation A48-T in NS4A. (A) Zoom view of the interaction interface of the CSFV NS3 protease domain (red) and the NS4A cofactor (blue) observed in the CSFV NS3/4A crystal structure (adapted from (Dubrau et al., 2017). The positions of the side chains of residues M132 in NS3, L45, Y47 and A48 in the NS4A kink region are highlighted with arrows in the respective colors. The PDB entry used is 5LKL (14). (B) Schematic representation of derivatives of CSFV NS2-Ubi-NS3 encoding the indicated mutations 2/V439-D, 2/T444-V, 3/M132-A, 4A/L45-A, 4A/Y47-A, 4A/A48-T and 5B/D280-G. (C) SK6 cells were electroporated with the indicated full length RNAs. At 48 h pe viral supernatants were harvested and analyzed for viral titers by limited dilution assay as TCID$_{50}$/ml. In addition, infections of SK6 cells were performed at MOI 0.1 followed by titer determination of cell culture supernatants collected at 72 h pi. Mean values and standard deviations of three experiments are depicted. N.d., not determined.

978 **Tables**

979 **TABLE 1** Overview of all mutations present in CSFV NS2-IRES-NS3$_{sc.}$ [a]

Nucleotide	AA in the viral polyprotein	viral protein	AA in the viral protein	Base exchange	Name or type of mutation
2101	577	E1	A83	G→A	E1/AT
2700	776	E2	S87	C→G	silent
4207	1279	NS2	Q147	C→A	2/QK
5085	1517	NS2	V439	T→A	2/VD
4998[b]	1576	NS2	T444	A→G	2/TV
4999[b]	1576	NS2	T444	C→T	2/TV
5533[b]	1721	NS3	M132	A→G	3/MA
5534[b]	1721	NS3	M132	T→C	3/MA
6292	1974	NS3	L385	T→A	3/LI
7330	2320	NS4A	A48	G→A	4A/A48-T
10751	3460	NS5B	D280	A→G	5B/DG

980 [a] Nucleotide and amino acid positions correspond to CSFV strain Alfort/Tuebingen (accession number: J04358.2).
981 [b] Positions were mutated before cell culture passage to introduce 2/T444-V and 3/M132-A into CSFV NS2-IRES-
982 NS3.

TABLE 1 Overview of all mutations present in CSFV NS2-IRES-NS3$_{sc.}$[a]

Nucleotide	AA in the viral polyprotein	viral protein	AA in the viral protein	Base exchange	Name or type of mutation
2101	577	E1	A83	G→A	E1/AT
2700	776	E2	S87	C→G	silent
4207	1279	NS2	Q147	C→A	2/QK
5085	1517	NS2	V439	T→A	2/VD
4998[b]	1576	NS2	T444	A→G	2/TV
4999[b]	1576	NS2	T444	C→T	2/TV
5533[b]	1721	NS3	M132	A→G	3/MA
5534[b]	1721	NS3	M132	T→C	3/MA
6292	1974	NS3	L385	T→A	3/LI
7330	2320	NS4A	A48	G→A	4A/A48-T
10751	3460	NS5B	D280	A→G	5B/DG

[a] Nucleotide and amino acid positions correspond to CSFV strain Alfort/Tuebingen (accession number: J04358.2).
[b] Positions were mutated before cell culture passage to introduce 2/T444-V and 3/M132-A into CSFV NS2-IRES-NS3.

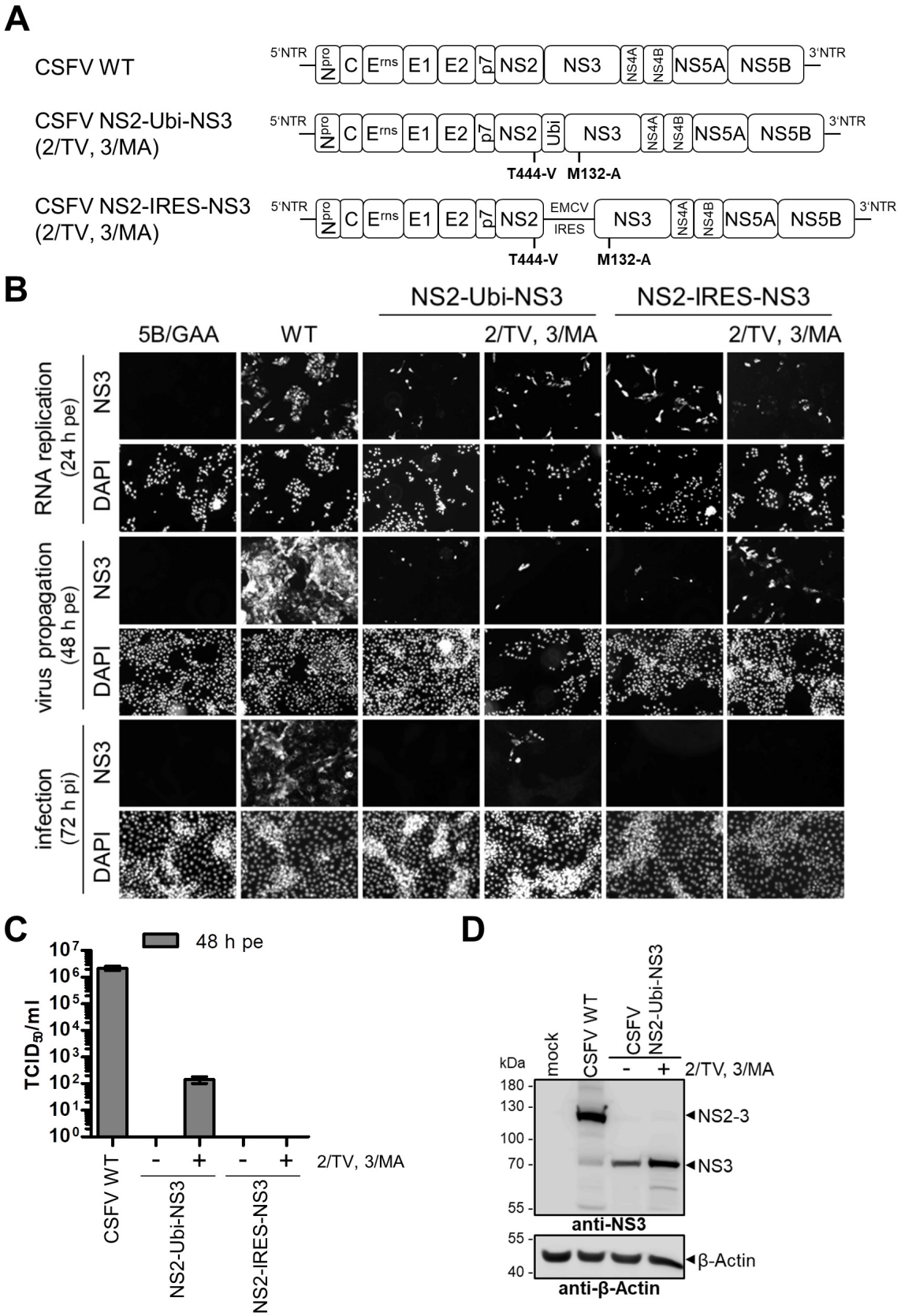

Figure 1

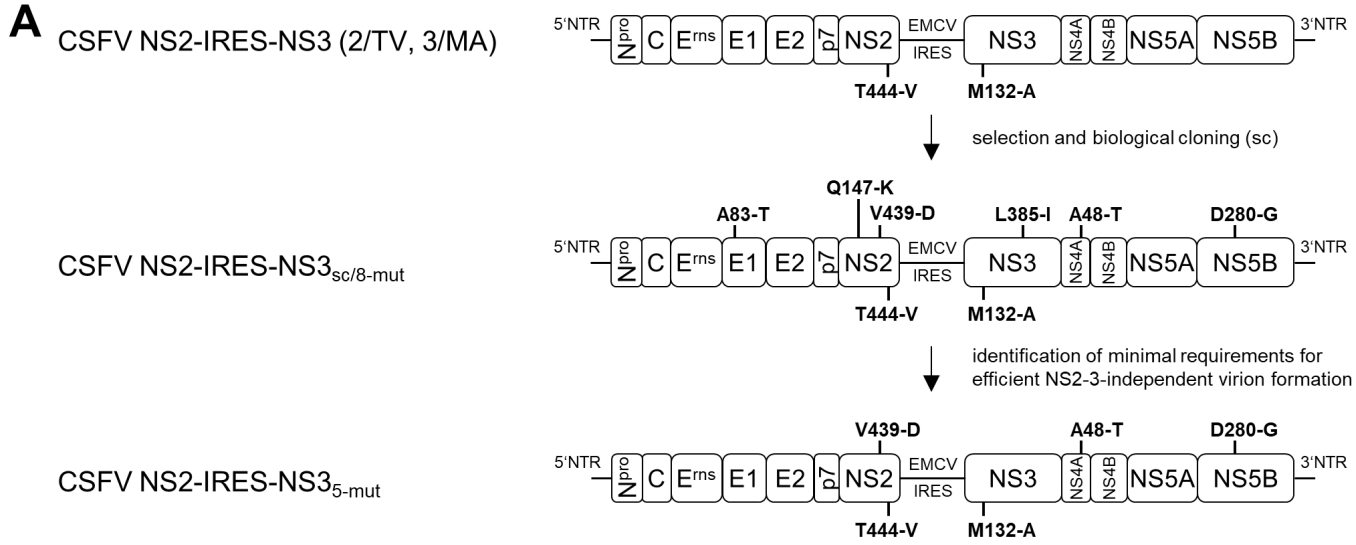

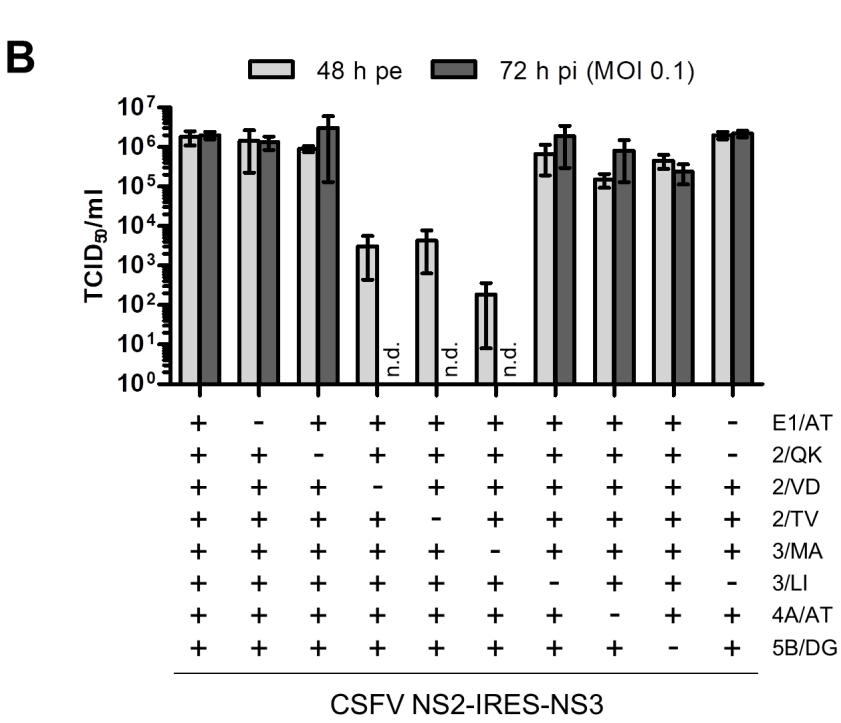

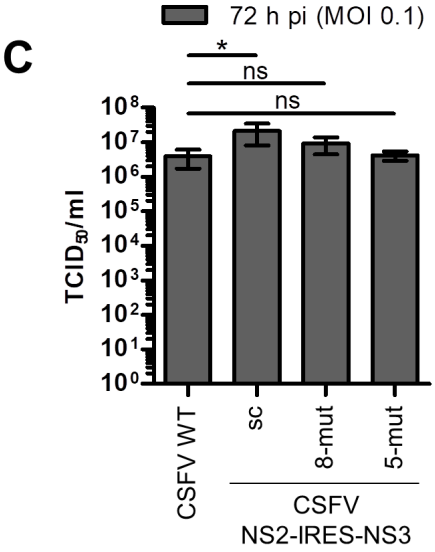

Figure 2

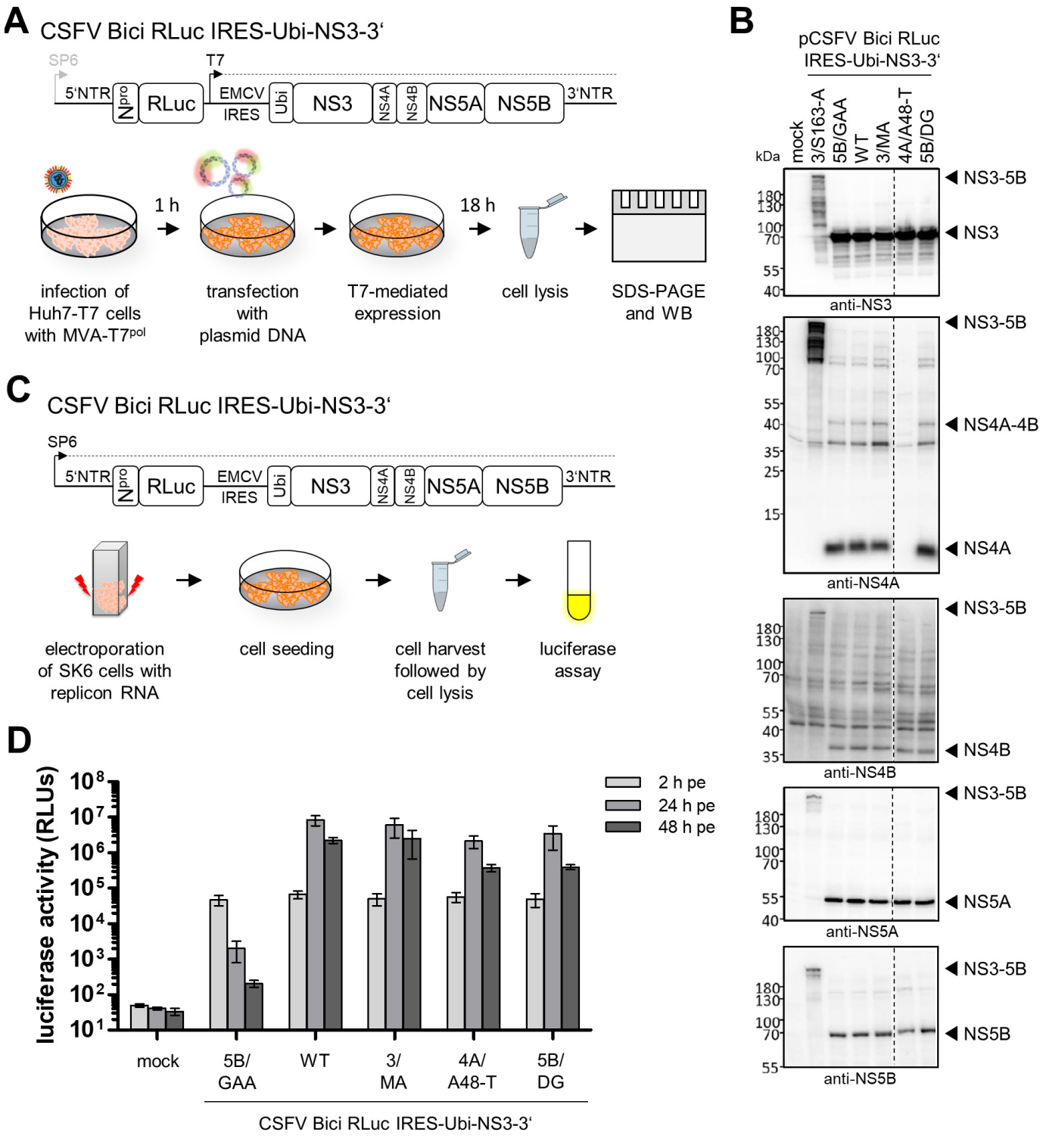

Figure 3

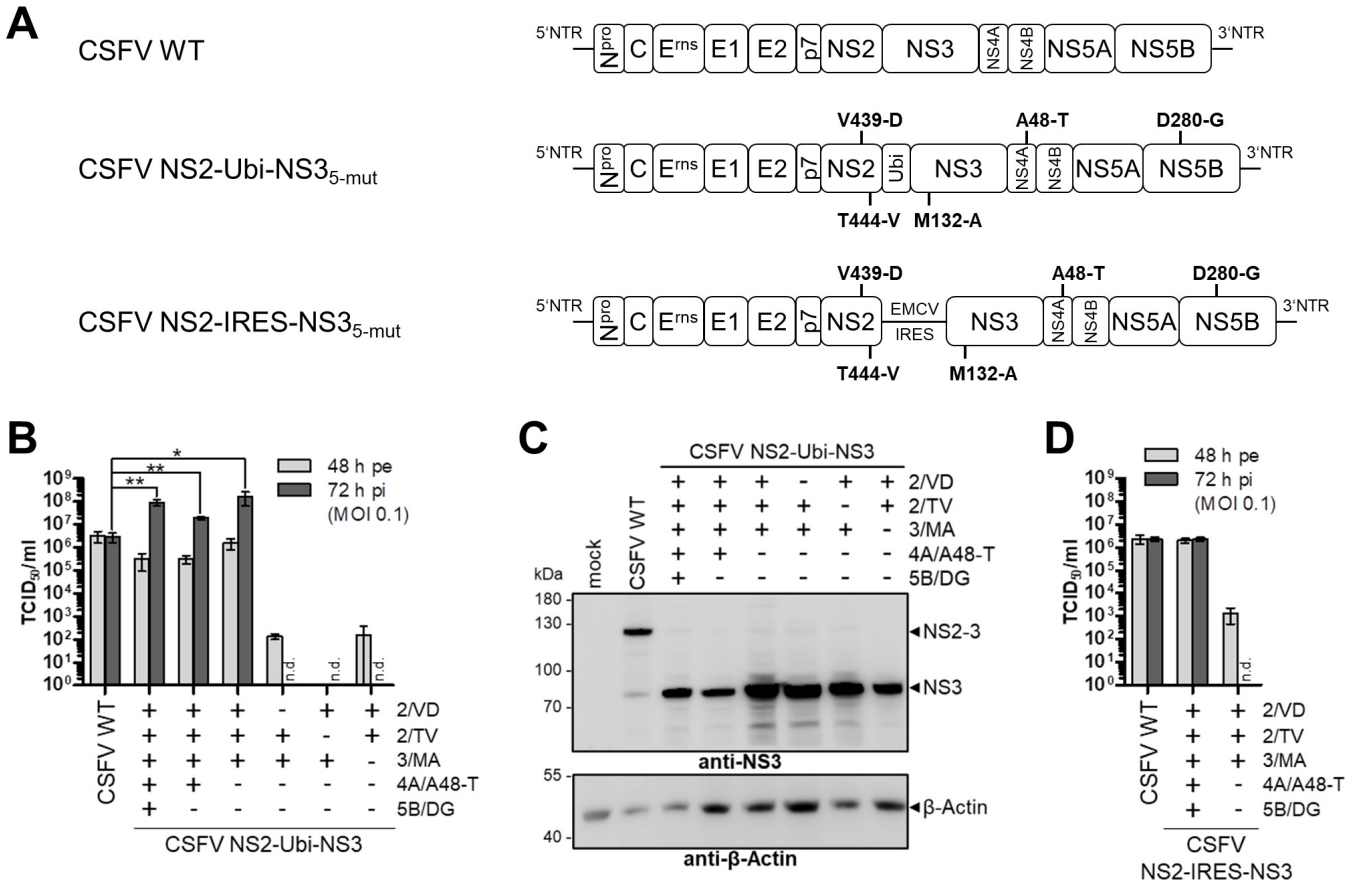

Figure 4

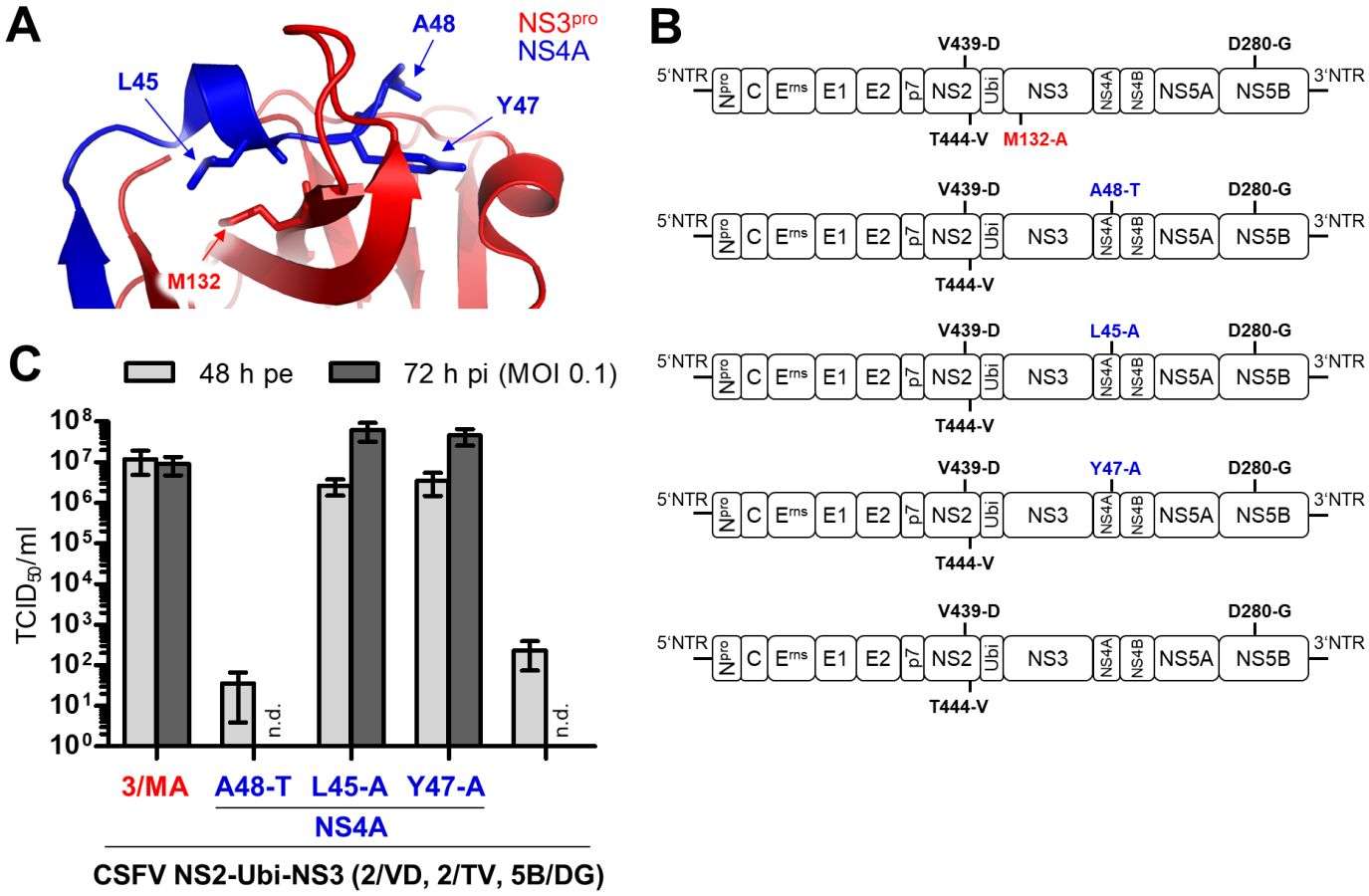

Figure 5